Constructing Explicit Decision Boundaries for the Optimization and Design of Cylindrical Implosion Experiments

W. P. Gammel[1,2], S. Missoum[1], J.P. Sauppe[2], B. Pidaparthi[1], and J.W. Jacobs[1]
[1]University of Arizona, [2]Los Alamos National Laboratory

Summary

1. We examine cylindrical implosion experiments modeled by 1D xRAGE[1,2] simulations.
2. Mikaelian's linear theory for stratified cylindrical targets is implemented for 1D xRAGE simulations. (K.O. Mikaelian, *Phys. Fluids* **17.9** (2005) 094105)
3. A Support Vector Machine Approach (SVM) is implemented for regime identification of perturbation growth based on target parameters.
4. The SVM boundary is used to identify parameter values leading to freeze-out conditions.

1. M. Gittings, Comp. Sci. Discovery 1.1 (2008) 015005, 2. B.M Haines, Phys. Plasmas 24.5 (2017) 052701

We are using cylindrical targets to diagnose hydrodynamic instability growth in convergent geometry.

- Inertial confinement fusion (ICF) capsule implosions suffer from hydrodynamic instabilities, which are modified in convergent geometry by Bell-Plesset[1,2] (BP) effects.
- Instabilities can compromise target integrity, or quench the hot-spot before maximum gain is achieved in fuel targets. Therefore, understanding and mitigating instability growth is crucial to improving target performance.

Cylindrical implosion experiments are used to directly measure instability growth: **Convergence + Diagnostic Access**

We examine the slow deceleration period of instability growth during these impulsively driven cylindrical implosions.

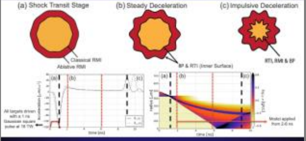

Mikaelian[1] extends linear theory to consider instability growth at multiple interfaces but in the absence of material compressibility.

- Evolution of the perturbation is dependent upon the radial, velocity, and acceleration trajectories.
- Incompressible: $\rho_{1,2}(t) = \rho_{1,2}(0)\exp[\gamma_\rho t] \rightarrow \gamma_\rho = 0$
- In its simplest form Mikaelian's model the takes form:

$\eta_{in/out}(t)$=inner/outer surface amplitude

$$\frac{d^2}{dt^2}\left(\frac{\eta_{out}+\eta_{in}}{2}\right) = -2\frac{\ddot{R}}{\Delta R}(\eta_{out}-\eta_{in})$$

$$\frac{d^2}{dt^2}\left[\frac{R}{\Delta R}(\eta_{out}-\eta_{in})\right] = \ddot{R}\left[2\frac{\eta_{out}-\eta_{in}}{\Delta R} - (m^2-1)\frac{\eta}{R}\right]$$

- This is valid only when $\Delta R \ll R$. A more general system was applied for the remainder of this work.

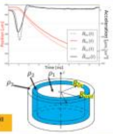

Mikaelian's model accounts for interface coupling effects, Bell Plesset Effects (BP), and instability growth from the RTI.

1. K. O. Mikaelian, *Phys. Fluids* **17.9** (2005) 094105.

Three behavioral patterns were observed as the ablator thickness and fill density were varied.

- All other parameters were held fixed to reduce the dimension of the design space.

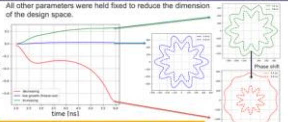

Note: To the author's knowledge, freeze-out of instability growth from the RTI has not yet been well-studied in relation to convergent targets

1. K. O. Mikaelian, *Phys. Fluids* **17.9** (2005) 094105.

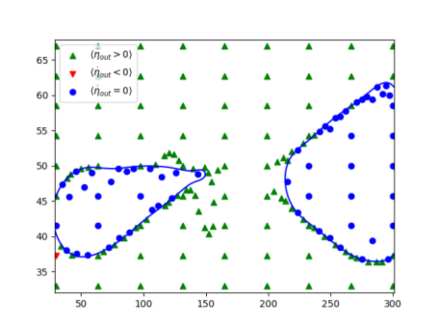

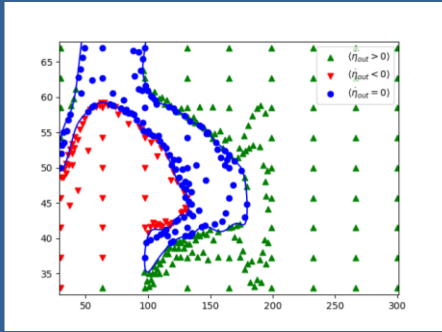

Above: SVM decision boundaries constructed for a 2D subspace of cylindrical target design parameters successfully isolate parameter combinations for which freeze-out is predicted to occur on the inner (left) or outer (right) surface of the Al marker layer.

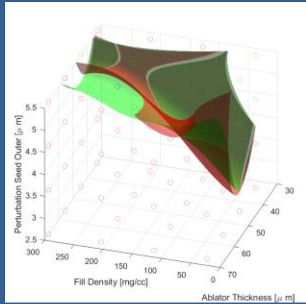

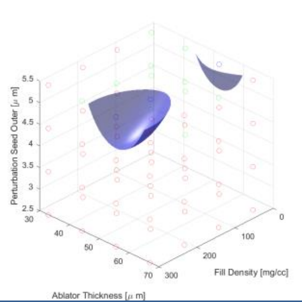

Above: Extensions of the decision boundary to higher dimensional parameter space is expected to provide further insight into which parameters (or combinations thereof) have the most appreciable effect on the behavior of the RTI.

The Support Vector Machine (SVM) is used to classify regions of parameter space.

The main idea:
For binary classification the SVM separates the data into two classes (positive / negative).

SVM has several features which make it a powerful tool for pattern recognition and classification:

- Multi-dimensionality.
- Ability to identify disjoint regions.

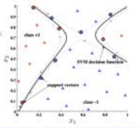

A. Basudhar, S. Missoum, **Computers & Structures 86** (2008)

In our problem, the three behavioral patterns of instability growth that arise from parameter modulation, form 3 unique classes of data.

Three classes of data arise as target parameters are varied:

- (1) Increasing: $\left(\frac{d\eta}{dt}\right) > 0$
- (2) Freeze-out: $\left(\frac{d\eta}{dt}\right) = 0$
- (3) Decreasing: $\left(\frac{d\eta}{dt}\right) < 0$

Class of data determined by applying Mikaelian's model to a unique 1D xRAGE simulation.

We use SVM as a <u>binary</u> classifier with three possible classes.

Two separate classifiers:

- Increasing vs Freeze out & Decreasing
- Decreasing vs Increasing & Freeze out

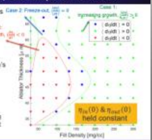

The region between the two decision boundaries is where we predict that freeze-out will occur for the chosen subset of parameter space.

- Ideally we want to see low amplitude growth on both the inner and outer surface of the marker layer.
- Here, the initial seed on the inner and outer surface of the marker layer is held fixed, and the ablator thickness and fill density are varied.

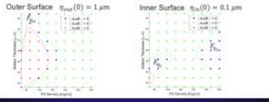

In order to construct an accurate decision boundary, additional points need to be populated along the boundary, in sparse regions of space.

- An adaptive sampling algorithm[1] is introduced to improve the accuracy of the decision boundary.
- Points are selected to reduce sparsity while improving the SVM classification.
  - A set of N points is generated over our space uniformly randomly
  - Fraction of convergence points for which there is a change of sign between two successive iterations is calculated. If fraction is less than $\epsilon_1 = 4.0\times10^{-3}$, algorithm ends.

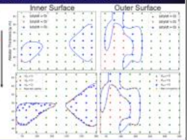

1. A. Basudhar, S. Missoum, *Computers and Structures 86* (2008)

The probability that uncertainty at a given point causes perturbation growth to deviate away from freeze-out is calculated.

Samples are selected from a multivariate normal distribution:

$$\mu = [x, y] \text{ and } \Sigma = \begin{bmatrix}\sigma_x^2 & 0 \\ 0 & \sigma_y^2\end{bmatrix}$$

Adaptive Sampling/Grid Point

Pt.	Ablator Thickness	Fill Density	Probability Freeze-Out condition not met
1	47.95 μm	146.3 mg/cc	0.008
2	47.37 μm	168.8 mg/cc	0.251
3	58.73 μm	69.6 mg/cc	0.558

The probability the freeze out condition is not met is:

Non-Freeze-out samples, Monte Carlo samples

$$P_{nf} = \frac{N_f}{N_{MCS}} = \frac{1}{N_{MCS}}\sum_{i=1}^{N_{MCS}} I_s(x_i)$$

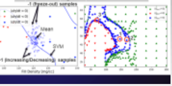

LA-UR-22-20820

This work performed under the auspices of the U.S. Department of Energy by Lawrence Livermore National Laboratory under Contract DE-AC52-07NA27344.